JOURNAL OF GUIDANCE, CONTROL, AND DYNAMICS
Vol. 32, No. 3, May–June 2009

Engineering Notes

ENGINEERING NOTES are short manuscripts describing new developments or important results of a preliminary nature. These Notes should not exceed 2500 words (where a figure or table counts as 200 words). Following informal review by the Editors, they may be published within a few months of the date of receipt. Style requirements are the same as for regular contributions (see inside back cover).

Effect of Kinematic Rotation-Translation Coupling on Relative Spacecraft Translational Dynamics

Shay Segal* and Pini Gurfil†
Technion—Israel Institute of Technology, 32000 Haifa, Israel

DOI: 10.2514/1.39320

I. Introduction

ACCURATE modeling of the differential translation and rotation between two spacecraft is essential for cooperative distributed space systems, spacecraft formation flying (SFF), rendezvous, and docking. High-fidelity relative motion modeling, as opposed to absolute motion modeling, is particularly important for autonomous missions [1].

Point-mass models for relative spacecraft translational motion have been extensively studied over the past 50 years, since Clohessy and Wiltshire (CW) presented a rendezvous model for a circular reference orbit and a spherical Earth [2]. Following the work of Clohessy and Wiltshire, variants on the point-mass model were developed, such as generalizations to elliptic reference orbits [3–5] and an oblate Earth [6,7].

The growing interest in SFF motivated the research of relative spacecraft motion modeling, yielding more accurate and complete equations and solutions for perturbed relative motion [8–10]. However, most of the works focused on point-mass, 3 degrees-of-freedom (DOF) spacecraft. Obviously, performing a space mission that consists of several cooperative space vehicles requires modeling the relative rotational motion in addition to the relative translation, that is, 6-DOF models.

Models for the relative motion of 6-DOF spacecraft have gained attention in the literature only in recent years. Among the first to suggest treating the spacecraft relative angular velocity in an SFF control problem were Pan and Kapila [11], who addressed the coupled translational and rotational dynamics of two spacecraft. By defining two body-fixed reference frames, one attached to the leader and the other attached to the follower, it was proposed [11] to use a two-part relative motion model: one that accounts for the relative translational dynamics of the body-fixed coordinate frame origins, and another that captures the relative attitude dynamics of the two body-fixed frames. A similar modeling approach was used for relative motion estimation [1]. In addition, tensorial equations of motion for a formation consisting of N spacecraft, each modeled as a rigid body, were derived [12]. However, only the absolute equations of motion were developed [12]; a relative version of these equations was not given. Moreover, a clear mathematical relationship between the developed models and the traditional nonlinear point-mass relative motion and CW models was not provided.

The coupling between the translational and rotational motion in the aforementioned models [1,11] was induced by gravity torques. The kinematic coupling, which is essentially a projection of the rotational motion about the center of mass (c.m.) onto the relative translational configuration space, was neglected. It is this kinematic coupling that the current paper is concerned with.

In general, rigid-body dynamics can be represented as translation of the c.m. and rotation about the c.m. [13]. Thus, spacecraft relative motion must be composed by combining the relative translational and rotational dynamics of *arbitrary* points on the spacecraft. Whenever one of these points does not coincide with the spacecraft's c.m., a kinematic coupling between the rotational and translational dynamics of these points is obtained.

The purpose of this paper is to quantify the kinematic coupling effect and to show that this effect is key for high-precision modeling of tight SFF, rendezvous, and docking. This effect is also important in vision-based relative attitude and position control, where arbitrary feature points on a target vehicle are to be tracked. Given two rigid-body spacecraft, the model presented herein is formulated in a general manner that describes the motion between any two arbitrary points on the spacecraft. The relative translational motion is then generated by both the spacecraft orbital motion and the rotation about the c.m.

In addition, this paper provides a CW-like approximation of the relative motion that includes the kinematic coupling. This new approximation is aimed at alleviating an apparent contradiction in linearized relative motion theories: to obtain linear equations of motion, the spacecraft are assumed to operate in close proximity. However, if the spacecraft are close to each other, then they can no longer be treated as point masses, because the spacecraft shape and size affects the relative translation between off-c.m. points. This effect is accentuated as the distances between spacecraft decrease.

The remainder of this paper is organized as follows. First, a background on the relative position and attitude dynamics is given. Then, a new coupled relative spacecraft motion model is presented. The newly developed model is then examined in a simulation.

II. Background

Consider two rigid-body spacecraft orbiting the Earth. One is a leader L and the other is a follower F. Based on the approach of previous studies [1,11], relative motion modeling starts by writing separate rotational and translational models. In the development of these models, the following coordinate systems are used: $\mathcal{I}$, the standard Earth-centered, inertial, Cartesian right-hand reference frame; $\mathcal{L}$, a local-vertical, local-horizontal Euler–Hill reference frame fixed to the leader spacecraft's c.m., with $\hat{\mathbf{x}}$ being a unit vector directed from the spacecraft radially outward, $\hat{\mathbf{z}}$ normal to the leader orbital plane, and $\hat{\mathbf{y}}$ completing the setup; $\mathcal{L}$, a Cartesian right-hand body-fixed reference frame attached to the leader spacecraft's c.m.; and $\mathcal{F}$, a Cartesian right-hand body-fixed reference frame attached to the follower spacecraft's c.m. In the following discussion, we assume that the orbital frame $\mathcal{L}$ is aligned with the body-fixed frame $\mathcal{L}$.

Received 24 June 2008; revision received 26 January 2009; accepted for publication 26 January 2009.

*Graduate Student, Faculty of Aerospace Engineering; shai@aerodyne.technion.ac.il.

†Senior Lecturer, Faculty of Aerospace Engineering; pgurfil@technion.ac.il. Associate Fellow AIAA.

A. Relative Translational Dynamics

Based on Newton's laws, the equations of motion for the leader and the follower in the absence of perturbing forces are

$$\ddot{\mathbf{r}}_L = -\frac{\mu}{r_L^3}\mathbf{r}_L, \qquad \ddot{\mathbf{r}}_F = -\frac{\mu}{r_F^3}\mathbf{r}_F \tag{1}$$

where $\mathbf{r}_L \in \mathbb{R}^3\backslash\{\mathbf{0}\}$ and $\mathbf{r}_F \in \mathbb{R}^3\backslash\{\mathbf{0}\}$ are the respective c.m. position vectors of L and F in $\mathcal{I}$, and μ is Earth's gravitational constant. The magnitudes of the position vectors are given by

$$r_L = \|\mathbf{r}_L\|_2 = \frac{a_L(1-e_L^2)}{1+e_L\cos f_L}, \qquad r_F = \|\mathbf{r}_F\|_2 = \frac{a_F(1-e_F^2)}{1+e_F\cos f_F} \tag{2}$$

where a_L and a_F are the semimajor axes, e_L and e_F are the eccentricities, and the variables f_L and f_F are the true anomalies of L and F, respectively. By defining the relative position vector as $\boldsymbol{\rho} = \mathbf{r}_L - \mathbf{r}_F = [x, y, z]^T \in \mathbb{R}^3$, the transitional dynamics of F relative to L, resolved in $\mathcal{L}$, can be written as [14]

$$\ddot{x} - 2\dot{f}_L\dot{y} - \ddot{f}_L y - \dot{f}_L^2 x = -\frac{\mu(r_L+x)}{[(r_L+x)^2+y^2+z^2]^{\frac{3}{2}}} + \frac{\mu}{r_L^2} \tag{3a}$$

$$\ddot{y} + 2\dot{f}_L\dot{x} + \ddot{f}_L x - \dot{f}_L^2 y = -\frac{\mu y}{[(r_L+x)^2+y^2+z^2]^{\frac{3}{2}}} \tag{3b}$$

$$\ddot{z} = -\frac{\mu z}{[(r_L+x)^2+y^2+z^2]^{\frac{3}{2}}} \tag{3c}$$

where the orbital angular velocity of the leader is given by

$$\dot{f}_L = \sqrt{\frac{\mu}{a_L^3(1-e_L^2)^3}}(1+e_L\cos f_L)^2 \tag{4}$$

and the orbital angular acceleration satisfies

$$\ddot{f}_L = \frac{-2\dot{r}_L\dot{f}_L}{r_L} \tag{5}$$

Thus, the relative translational dynamics are described by a set of nonlinear ordinary differential equations for the eight-dimensional state vector $[\boldsymbol{\rho}^T, \dot{\boldsymbol{\rho}}^T, f_L, \dot{f}_L]^T$.

B. Relative Rotational Dynamics

The purpose of the following development is to derive a model that describes the rotational motion of F relative to L, expressed in terms of relative quantities and the angular velocity of L. To that end, we denote the angular velocity of F relative to L, $\boldsymbol{\omega} \in \mathbb{R}^3$, so that

$$\boldsymbol{\omega} \triangleq \boldsymbol{\omega}_F - \boldsymbol{\omega}_L \tag{6}$$

where $\boldsymbol{\omega}_L$ and $\boldsymbol{\omega}_F$ are the angular velocities of F and L, respectively, in a given reference frame.

In the remainder of paper, the notation $\mathbf{A}_N$ stands for the vector $\mathbf{A}$ expressed in the N frame, and $\mathrm{d}\mathbf{A}/\mathrm{d}t|_N$ denotes the time derivative of $\mathbf{A}$ in the reference frame N.

The attitude of F relative to L will be parameterized using the Euler parameters q_1, q_2, q_3, and q_4. The rotation matrix D, which transforms a vector from frame $\mathcal{F}$ to frame $\mathcal{L}$, can be expressed in terms of the quaternion $\mathbf{q} = [q_1, q_2, q_3, q_4]^T$ as

$$D(\mathbf{q}) = \begin{bmatrix} q_1^2-q_2^2-q_3^2+q_4^2 & 2(q_1q_2-q_3q_4) & 2(q_1q_3+q_2q_4) \\ 2(q_1q_2+q_3q_4) & -q_1^2+q_2^2-q_3^2+q_4^2 & 2(q_2q_3-q_1q_4) \\ 2(q_1q_3-q_2q_4) & 2(q_2q_3+q_1q_4) & -q_1^2-q_2^2+q_3^2+q_4^2 \end{bmatrix} \tag{7}$$

and the attitude kinematics of F relative to L can be described using the quaternion kinematic equations

$$\dot{\mathbf{q}} = \tfrac{1}{2}Q(\mathbf{q})\boldsymbol{\omega}^{\mathcal{F}} \tag{8}$$

where

$$Q = \begin{bmatrix} q_4 & -q_3 & q_2 \\ q_3 & q_4 & -q_1 \\ -q_2 & q_1 & q_4 \\ -q_1 & -q_2 & -q_3 \end{bmatrix} \tag{9}$$

The attitude dynamics of F relative to L, expressed in $\mathcal{L}$, will now be derived according to the guidelines of [11]. First, a differentiation of Eq. (6) with respect to the inertial frame leads to

$$\left.\frac{\mathrm{d}\boldsymbol{\omega}}{\mathrm{d}t}\right|_{\mathcal{I}} = \left.\frac{\mathrm{d}\boldsymbol{\omega}_F}{\mathrm{d}t}\right|_{\mathcal{I}} - \left.\frac{\mathrm{d}\boldsymbol{\omega}_L}{\mathrm{d}t}\right|_{\mathcal{I}} \tag{10}$$

Equation (10) leads in a straightforward manner to

$$\left(\left.\frac{\mathrm{d}\boldsymbol{\omega}}{\mathrm{d}t}\right|_{\mathcal{L}}\right)^{\mathcal{L}} = D(\mathbf{q})\left(\left.\frac{\mathrm{d}\boldsymbol{\omega}_F}{\mathrm{d}t}\right|_{I}\right)^{\mathcal{F}} - \left(\left.\frac{\mathrm{d}\boldsymbol{\omega}_L}{\mathrm{d}t}\right|_{I}\right)^{\mathcal{L}} - (\tilde{\boldsymbol{\omega}}_L)^{\mathcal{L}}\boldsymbol{\omega}^{\mathcal{L}} \tag{11}$$

where, for any vector $\mathbf{v} = [v_1, v_2, v_3]^T$,

$$\tilde{\mathbf{v}} = \begin{bmatrix} 0 & -v_3 & v_2 \\ v_3 & 0 & -v_1 \\ -v_2 & v_1 & 0 \end{bmatrix} \tag{12}$$

Multiplying Eq. (11) by the inertia tensor of the leader, $\mathbf{I}_L \in \mathbb{R}^{3\times3}$, gives

$$\mathbf{I}_L\left(\left.\frac{\mathrm{d}\boldsymbol{\omega}}{\mathrm{d}t}\right|_{\mathcal{L}}\right)^{\mathcal{L}} = \mathbf{I}_L D(\mathbf{q})\left(\left.\frac{\mathrm{d}\boldsymbol{\omega}_F}{\mathrm{d}t}\right|_{\mathcal{F}}\right)^{\mathcal{F}} - \mathbf{I}_L\left(\left.\frac{\mathrm{d}\boldsymbol{\omega}_L}{\mathrm{d}t}\right|_{\mathcal{L}}\right)^{\mathcal{L}} - \mathbf{I}_L(\tilde{\boldsymbol{\omega}}_L)^{\mathcal{L}}\boldsymbol{\omega}^{\mathcal{L}} \tag{13}$$

If $\mathbf{H}$ is the total angular momentum of a rigid body and $\mathbf{N}$ is an external torque on the body, then, for the follower,

$$\left.\frac{\mathrm{d}\mathbf{H}_F}{\mathrm{d}t}\right|_{\mathcal{I}} = \left.\frac{\mathrm{d}\mathbf{H}_F}{\mathrm{d}t}\right|_{\mathcal{F}} + \boldsymbol{\omega}_F \times \mathbf{H}_F = \mathbf{N}_F \tag{14}$$

and for the leader

$$\left.\frac{\mathrm{d}\mathbf{H}_L}{\mathrm{d}t}\right|_{\mathcal{I}} = \left.\frac{\mathrm{d}\mathbf{H}_L}{\mathrm{d}t}\right|_{\mathcal{L}} + \boldsymbol{\omega}_L \times \mathbf{H}_L = \mathbf{N}_L \tag{15}$$

Since $\mathbf{H}_L = \mathbf{I}_L\boldsymbol{\omega}_L$ and $\mathbf{H}_F = \mathbf{I}_F\boldsymbol{\omega}_F$, with $\mathbf{I}_F \in \mathbb{R}^{3\times3}$ being the inertia tensor of the follower,

$$\mathbf{I}_F\left.\frac{\mathrm{d}\boldsymbol{\omega}_F}{\mathrm{d}t}\right|_{\mathcal{I}} = \mathbf{I}_F\left.\frac{\mathrm{d}\boldsymbol{\omega}_F}{\mathrm{d}t}\right|_{\mathcal{F}} + \boldsymbol{\omega}_F \times \mathbf{I}_F\boldsymbol{\omega}_F = \mathbf{N}_F \tag{16}$$

and

$$\mathbf{I}_L\left.\frac{\mathrm{d}\boldsymbol{\omega}_L}{\mathrm{d}t}\right|_{\mathcal{I}} = \mathbf{I}_L\left.\frac{\mathrm{d}\boldsymbol{\omega}_L}{\mathrm{d}t}\right|_{\mathcal{L}} + \boldsymbol{\omega}_L \times \mathbf{I}_L\boldsymbol{\omega}_L = \mathbf{N}_L \tag{17}$$

Now, substituting Eqs. (16) and (17) into Eq. (13) gives

$$\mathbf{I}_L\left(\left.\frac{\mathrm{d}\boldsymbol{\omega}}{\mathrm{d}t}\right|_{\mathcal{L}}\right)^{\mathcal{L}} = \mathbf{I}_L D(\mathbf{q})\mathbf{I}_F^{-1}[\mathbf{N}_F - \boldsymbol{\omega}_F^{\mathcal{F}} \times \mathbf{I}_F\boldsymbol{\omega}_F^{\mathcal{F}}] - \mathbf{I}_L\boldsymbol{\omega}_L^{\mathcal{L}} \times \boldsymbol{\omega}^{\mathcal{L}} - [\mathbf{N}_L - \boldsymbol{\omega}_L^{\mathcal{L}} \times \mathbf{I}_L\boldsymbol{\omega}_L^{\mathcal{L}}] \tag{18}$$

or

$$\mathbf{I}_L\dot{\boldsymbol{\omega}} = \mathbf{I}_L D\mathbf{I}_F^{-1}[\mathbf{N}_F - D^T(\boldsymbol{\omega}^{\mathcal{L}} + \boldsymbol{\omega}_L^{\mathcal{L}}) \times \mathbf{I}_F D^T(\boldsymbol{\omega}^{\mathcal{L}} + \boldsymbol{\omega}_L^{\mathcal{L}})] - \mathbf{I}_L\boldsymbol{\omega}_L^{\mathcal{L}} \times \boldsymbol{\omega}^{\mathcal{L}} - [\mathbf{N}_L - \boldsymbol{\omega}_L^{\mathcal{L}} \times \mathbf{I}_L\boldsymbol{\omega}_L^{\mathcal{L}}] \tag{19}$$

Thus, the relative rotational kinematics and dynamics are described by Eqs. (8) and (19) for a seven-dimensional state vector $[\boldsymbol{\omega}, \mathbf{q}]$.

The complete relative motion is described by both the relative rotational and relative translational dynamics, which yields a system comprising a 15-element relative state vector $[\boldsymbol{\rho}, \dot{\boldsymbol{\rho}}, f, \dot{f}, \boldsymbol{\omega}, \mathbf{q}]$. In most recent studies, the coupling between the rotational and translation dynamics arises because of *external* torques; the most obvious example is the gravity gradient torque, which depends on altitude. In the following section, a different, *internal*, external-perturbations-independent coupling will be discussed; this coupling stems from the fact that relative motion equations can be written for any point on the spacecraft, not necessarily the c.m. Thus, an apparent translational motion of points on the follower spacecraft (that do not coincide with the c.m.) will result from rotation of the follower about its c.m.

III. Kinematically Coupled Relative Spacecraft Motion Model

Consider two arbitrary feature points located on the leader and follower spacecraft, as shown in Fig. 1. Let P_L^j be a point on the leader spacecraft body. Then, $\mathbf{P}_L^j = [P_{xL}^j, P_{yL}^j, P_{zL}^j]^T$ is a vector directed from the origin of the coordinate system $\mathcal{L}$ to the point P_L^j. In the special case where P_L^j coincides with the leader's spacecraft c.m., $\mathbf{P}_L^0 = [0, 0, 0]^T$. Similarly, P_F^i is an arbitrary point on the follower spacecraft. Thus, $\mathbf{P}_F^i = [P_{xF}^i, P_{yF}^i, P_{zF}^i]^T$ is a vector directed from the origin of the coordinate system $\mathcal{F}$ to the point P_F^i, and P_F^0 is a point located on the follower's spacecraft c.m., so that $\mathbf{P}_F^0 = [0, 0, 0]^T$. Let $\boldsymbol{\rho}_{ij}$ denote the relative position vector between point j on the leader and point i on the follower spacecraft. Then $\boldsymbol{\rho}_0$ is the relative position vector between the centers of mass of the spacecraft. By observing Fig. 1, one can note that the following relationship holds:

$$\boldsymbol{\rho}_{ij} = \boldsymbol{\rho}_0 + \mathbf{P}_F^i - \mathbf{P}_L^j \tag{20}$$

The first and second time derivatives of $\boldsymbol{\rho}_{ij}$ in $\mathcal{L}$ can be easily shown to reduce to

$$\dot{\boldsymbol{\rho}}_{ij} = \dot{\boldsymbol{\rho}}_0 + \boldsymbol{\omega} \times \mathbf{P}_F^i \tag{21}$$

$$\ddot{\boldsymbol{\rho}}_{ij} = \ddot{\boldsymbol{\rho}}_0 + \dot{\boldsymbol{\omega}} \times \mathbf{P}_F^i + \boldsymbol{\omega} \times (\boldsymbol{\omega} \times \mathbf{P}_F^i) \tag{22}$$

The translational motion model describing the relative motion between the leader and follower spacecraft centers of mass, that is, a model for the case where $\mathbf{P}_F^i = \mathbf{P}_L^j = \mathbf{0}$, is usually written in the form $\ddot{\boldsymbol{\rho}}_0 = \mathbf{g}_0(\boldsymbol{\rho}_0, r_L, \dot{f}_L, \ddot{f}_L)$, as shown in Eqs. (3). We have developed a more general model, in which $\ddot{\boldsymbol{\rho}}_{ij} = \mathbf{g}(\boldsymbol{\rho}_{ij}, r_L, \dot{f}_L, \ddot{f}_L, \boldsymbol{\omega}, \dot{\boldsymbol{\omega}}, \mathbf{P}_F^i, \mathbf{P}_L^j)$. This model is obtained by 1) writing Eqs. (20–22) in terms of the vector components in frame $\mathcal{L}$, that is, $\boldsymbol{\rho}_0 = [x_0, y_0, z_0]^T, \boldsymbol{\omega} = [\omega_x, \omega_y, \omega_z]^T$, and 2) substituting the resulting scalar equations into Eqs. (3). This process yields the following general description of the translational motion between any arbitrary points $P^i \in F$ and $P^j \in L$ in the absence of perturbing forces:

$$\begin{aligned}
&\ddot{x}_{ij} - [\omega_y(\omega_x P_{yF}^i - \omega_y P_{xF}^i) + \omega_z(\omega_z P_{xF}^i - \omega_x P_{zF}^i)] - \dot{\omega}_y P_{zF}^i + \dot{\omega}_z P_{yF}^i \\
&\quad - 2\dot{f}_L[\dot{y}_{ij} - (\omega_z P_{xF}^i + \omega_x P_{zF}^i)] + \ddot{f}_L(y_{ij} - P_{yF}^i + P_{yL}^j) - \dot{f}_L^2(x_{ij} - P_{xF}^i + P_{xL}^j) \\
&\quad = \frac{-\mu(r_L + x_{ij} - P_{xF}^i + P_{xL}^j)}{[(r_L + x_{ij} - P_{xF}^i + P_{xL}^j)^2 + (y_{ij} - P_{yF}^i + P_{yL}^j)^2 + (z_{ij} - P_{zF}^i + P_{zL}^j)^2]^{\frac{3}{2}}} + \frac{\mu}{r_L^2}
\end{aligned} \tag{23}$$

$$\begin{aligned}
&\ddot{y}_{ij} - [\omega_z(\omega_y P_{zF}^i - \omega_z P_{yF}^i) + \omega_x(\omega_x P_{yF}^i - \omega_y P_{xF}^i)] - \dot{\omega}_z P_{xF}^i + \dot{\omega}_x P_{zF}^i \\
&\quad + 2\dot{f}_L[\dot{x}_{ij} - (\omega_y P_{zF}^i + \omega_z P_{yF}^i)] + \ddot{f}_L(x_{ij} - P_{xF}^i - P_{xL}^j) - \dot{f}_L^2(y_{ij} - P_{yF}^i + P_{yL}^j) \\
&\quad = \frac{-\mu(y_{ij} - P_{yF}^i + P_{yL}^j)}{[(r_L + x_{ij} - P_{xF}^i + P_{xL}^j)^2 + (y_{ij} - P_{yF}^i + P_{yL}^j)^2 + (z_{ij} - P_{zF}^i + P_{zL}^j)^2]^{\frac{3}{2}}}
\end{aligned} \tag{24}$$

$$\begin{aligned}
&\ddot{z}_{ij} - [\omega_x(\omega_z P_{xF}^i - \omega_x P_{zF}^i) + \omega_y(\omega_y P_{zF}^i - \omega_z P_{yF}^i)] - \dot{\omega}_x P_{yF}^i + \dot{\omega}_y P_{xF}^i \\
&\quad = \frac{-\mu(z_{ij} - P_{zF}^i + P_{zL}^j)}{[(r_L + x_{ij} - P_{xF}^i + P_{xL}^j)^2 + (y_{ij} - P_{yF}^i + P_{yL}^j)^2 + (z_{ij} - P_{zF}^i + P_{zL}^j)^2]^{\frac{3}{2}}}
\end{aligned} \tag{25}$$

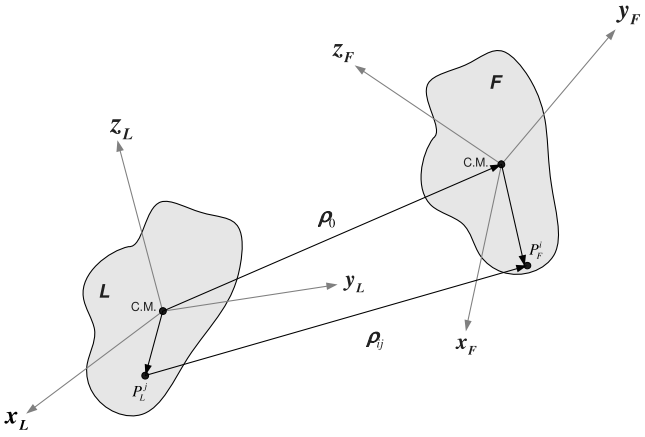

Fig. 1 Two rigid-body spacecraft with body-fixed reference frames.

These equations are coupled to the rotational motion Eqs. (8) and (19) through the components of the relative angular velocity vector $\boldsymbol{\omega}$. Therefore, the 6-DOF description of the rigid-body relative spacecraft motion is given by the following set of nonlinear coupled differential equations: Eqs. (4), (5), (8), (19), and (23–25).

An approximated set of translational equations of motion can be obtained using the same assumptions leading to the CW equations, that is, a circular reference orbit and a small relative distance compared to the orbital radius. It should be noted that these assumptions will lead to differential equations that are linear with respect to the relative position, and nonlinear with respect to the component of the relative angular velocity vector. Thus, by applying the CW rationale on Eqs. (23–25), the following approximate equations are obtained:

$$\dot{\mathbf{x}}_{\text{tr}} = A\mathbf{x}_{\text{tr}} + \mathbf{p} \tag{26}$$

where $\mathbf{x}_{\text{tr}} = [\boldsymbol{\rho}^T, \dot{\boldsymbol{\rho}}^T]^T$, $\dot{f}_L = n = \text{const}$,

$$A = \begin{bmatrix} 0 & 0 & 0 & 1 & 0 & 0 \\ 0 & 0 & 0 & 0 & 1 & 0 \\ 0 & 0 & 0 & 0 & 0 & 1 \\ 3n^2 & 0 & 0 & 0 & 2n & 0 \\ 0 & 0 & 0 & -2n & 0 & 0 \\ 0 & 0 & -n^2 & 0 & 0 & 0 \end{bmatrix} \tag{27}$$

and $\mathbf{p} = [0, 0, 0, p_1, p_2, p_3]^T$ is defined by

$$\begin{aligned} p_1 &\triangleq 3n^2(P^i_{xL} - P^j_{xF}) - 2n(\omega_z P^i_{xF} - \omega_x P^i_{zF}) \\ &\quad + [\omega_y(\omega_x P^i_{yF} - \omega_y P^i_{xF}) + \omega_z(\omega_z P^i_{xF} - \omega_x P^i_{zF})] \\ &\quad + \dot{\omega}_y P^i_{zF} - \dot{\omega}_z P^i_{yF} \\ p_2 &\triangleq 3n^2(P^i_{xL} - P^j_{xF}) - 2n(\omega_z P^i_{xF} - \omega_x P^i_{zF}) \\ &\quad + [\omega_y(\omega_x P^i_{yF} - \omega_y P^i_{xF}) + \omega_z(\omega_z P^i_{xF} - \omega_x P^i_{zF})] \\ &\quad + \dot{\omega}_y P^i_{zF} - \dot{\omega}_z P^i_{yF} \\ p_3 &\triangleq 3n^2(P^i_{xL} - P^j_{xF}) - 2n(\omega_z P^i_{xF} - \omega_x P^i_{zF}) \\ &\quad + [\omega_y(\omega_x P^i_{yF} - \omega_y P^i_{xF}) + \omega_z(\omega_z P^i_{xF} - \omega_x P^i_{zF})] \\ &\quad + \dot{\omega}_y P^i_{zF} - \dot{\omega}_z P^i_{yF} \end{aligned} \tag{28}$$

These terms result from the coupling to the rotational dynamics, and can be treated as a *kinematic perturbation*. However, this perturbation will always be present, regardless of the orbital altitude and external perturbations. It will be accentuated when the relative distances become small.

IV. Simulation

In this section, the new coupled relative motion models will be illustrated by numerically integrating trajectories of several feature points on a follower spacecraft relative to a leader spacecraft's c.m. Two cases are examined: a simulation of the fully coupled, nonlinear model (23–25) applied on an SFF mission in low-Earth orbit, and a simulation of the approximate model (26) for a rendezvous problem. In both cases, the inertia tensors of the leader and follower spacecraft satisfy $\mathbf{I}_L = \mathbf{I}_F = \mathbf{I} = \text{diag}[500, 550, 600]$ kgm^2.

A. Formation Flying Simulation

In the first scenario, a leader spacecraft is orbiting the Earth in an elliptic orbit with eccentricity $e_L = 0.05$, semimajor axis $a_L = 7170$ km, and inclination $I_L = 15$ deg. The argument of perigee of the leader satisfies $\omega_L = 340$ deg, the right ascension of the ascending node is $\Omega_L = 0$, and the initial true anomaly is $f_L(0) = 20$ deg. The nonlinear coupled motion model is then used to simulate the relative distances between three feature points on the follower spacecraft P^i_F, $i = 0, 1, 2$, and the leader spacecraft's c.m. P^0_L. The corresponding vectors are $\mathbf{P}^0_L = [0, 0, 0]^T$, $\mathbf{P}^0_F = [0, 0, 0]^T$, $\mathbf{P}^1_F = [1.5, 1.5, 0]^T$, and $\mathbf{P}^2_F = [-1.5, -1.5, 0]^T$ m. The initial conditions of the simulation are as follows:

$$\begin{aligned} &\boldsymbol{\rho}_0(0) = [25, 25, 50]^T \text{ m}, \qquad \dot{\boldsymbol{\rho}}_0(0) = [0, -0.0555, 0]^T \text{ m/s} \\ &\boldsymbol{\omega}(0) = [0.1\dot{f}_L(0), 0.1\dot{f}_L(0), 2\dot{f}_L(0)]^T \qquad \mathbf{q}(0) = [0, 0, 0, 1]^T \end{aligned} \tag{29}$$

where $\dot{f}_L(0) = 0.0656$ deg/s is calculated using Eq. (4). These initial conditions were chosen to satisfy the energy matching condition [8]

$$\begin{aligned} &\frac{1}{2}\{[\dot{x}_0(0) - \dot{f}_L(0)y_0(0) + \dot{r}_L(0)]^2 \\ &\quad + [\dot{y}_0(0) + \dot{f}_L(0)(x_0(0) + r_L(0))]^2 + \dot{z}^2_0(0)\} \\ &\quad - \frac{\mu}{\sqrt{[x_0(0) + r_L(0)]^2 + y^2_0(0) + z^2_0(0)}} = -\frac{\mu}{2a_L} \end{aligned} \tag{30}$$

guaranteeing bounded relative motion between the spacecraft in the formation.

The initial conditions for the feature points on the follower that do not coincide with the c.m. are calculated by applying Eqs. (20–22),

$$\begin{aligned} \boldsymbol{\rho}_{ij}(0) &= \boldsymbol{\rho}_0(0) + \mathbf{P}^i_F - \mathbf{P}^j_L \\ \dot{\boldsymbol{\rho}}_{ij}(0) &= \dot{\boldsymbol{\rho}}_0(0) + \boldsymbol{\omega}_0 \times (\mathbf{P}^i_F - \mathbf{P}^j_L), \qquad i = 1, 2, j = 0 \end{aligned} \tag{31}$$

which results in

$$\begin{aligned} \boldsymbol{\rho}_{10}(0) &= [26.5, 26.5, 50]^T \text{ m} \\ \dot{\boldsymbol{\rho}}_0(0) &= [-0.0034, -0.052, 0]^T \text{ m/s} \end{aligned} \tag{32}$$

$$\begin{aligned} \boldsymbol{\rho}_{20}(0) &= [23.5, 23.5, 50]^T \text{ m} \\ \dot{\boldsymbol{\rho}}_0(0) &= [0.034, -0.0589, 0]^T \text{ m/s} \end{aligned} \tag{33}$$

The results of the formation flying simulation for a single orbital period of the leader are depicted by Figs. 2 and 3. Figure 2 shows the position components of the selected feature point on the follower's body relative to the leader's c.m., that is, $\boldsymbol{\rho}_{10} = \boldsymbol{\rho}_0 + \mathbf{P}^1_F - \mathbf{P}^0_L$, $\boldsymbol{\rho}_{20} = \boldsymbol{\rho}_0 + \mathbf{P}^2_F - \mathbf{P}^0_L$, and $\boldsymbol{\rho}_0$ (the last vector represents the position of the follower's c.m. relative to the leader's c.m.). Figure 3 shows the deviation in the relative position of the feature points due to the coupling effect. These deviations are defined as $\Delta\boldsymbol{\rho}_1 = \boldsymbol{\rho}_{10} - \boldsymbol{\rho}_0$ and $\Delta\boldsymbol{\rho}_2 = \boldsymbol{\rho}_{20} - \boldsymbol{\rho}_0$.

Figure 2 clearly demonstrates that the relative position between the leader's c.m. and the chosen feature points on the follower depends upon the chosen points' location in the follower's body frame. Moreover, Fig. 3 shows that the relative motion between the leader's c.m. and feature points on the follower spacecraft that do not coincide with the follower's c.m. exhibit harmonic oscillations whose frequency is determined by the relative angular velocity. The magnitude of these oscillations depends on the location of the point in the follower's body frame. Evidently, this result is different from standard 6-DOF models, which do not take the kinematic coupling into consideration, that is, they neglect the effect of the relative rotation on the relative translation.

B. Rendezvous Simulation

In the second scenario, a leader spacecraft is orbiting the Earth in circular orbit, $e_L = 0$, with radius $a_L = 7170$ km, inclination of $I_L = 15$ deg, and node at $\Omega_L = 0$ deg. The initial true anomaly is $f_L(0) = 20$ deg. The approximate model (26) is used to simulate the relative distance between two feature points P^i_F, $i = 0$, 1, on the

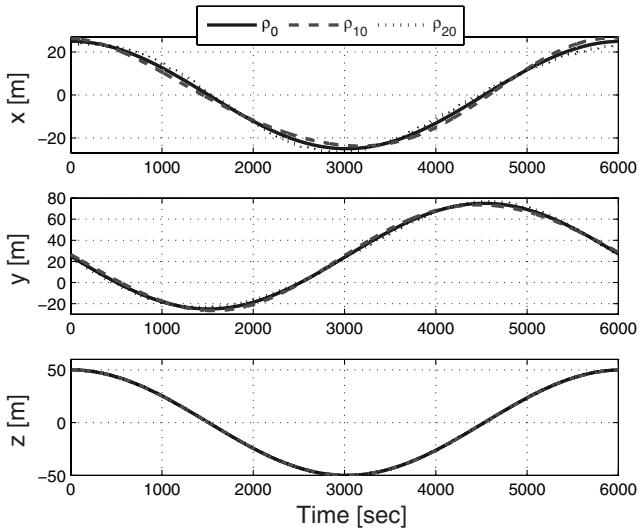

Fig. 2 Time histories of the position components of several feature points on the follower spacecraft relative to the leader's spacecraft center of mass.

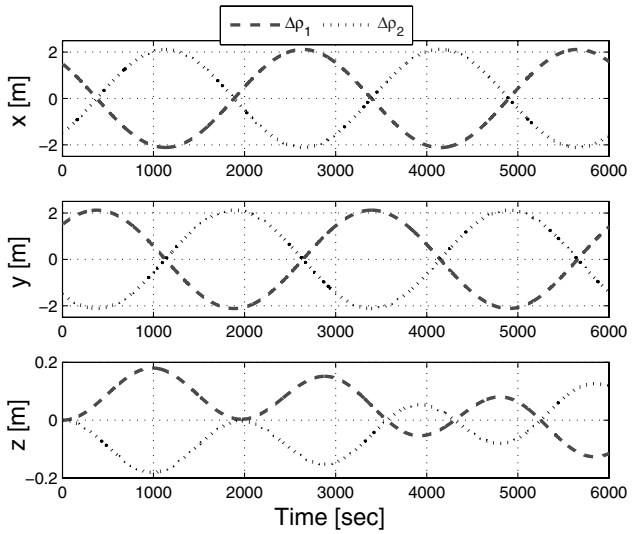

Fig. 3 Time histories of the relative displacement components of points on the follower spacecraft relative to the line joining the spacecraft centers of mass.

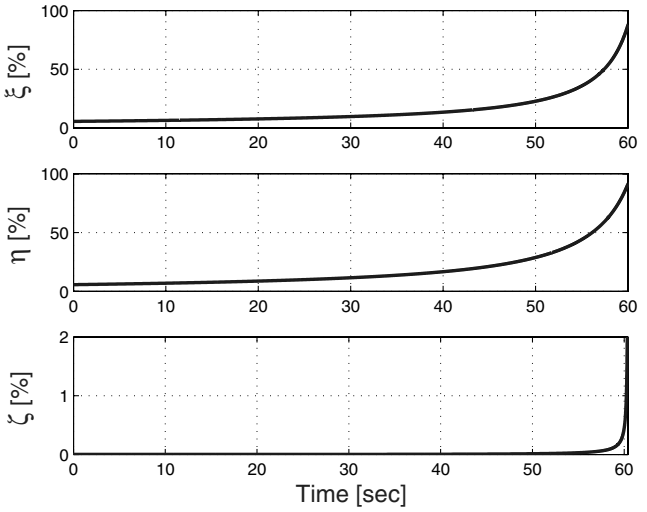

Fig. 5 Although the Clohessy–Wiltshire model is widely used for the final approach phase of rendezvous missions, this figure shows that the effect of rotational-translation kinematic coupling impairs the validity of the CW model.

follower spacecraft and the leader spacecraft's c.m. P_L^0. These points are selected as follows: the follower's c.m., with the position vector $\mathbf{P}_F^0 = [0, 0, 0]^T$ and $\mathbf{P}_F^1 = [1.5, 1.5, 0]^T$ m. Note that for $\boldsymbol{\rho}_0$, the approximate model (26) degenerates into the regular CW model. The initial conditions of the relative position and relative velocity where chosen so as to nullify the relative position $\boldsymbol{\rho}_0$ at the specified time $t_f = 0.01T = 60.42$ s, where $T = 2\pi\sqrt{a_L^3/\mu} = 100.7$ min. The resulting initial conditions are

$$\boldsymbol{\rho}_0(0) = [25, 25, 50]^T \text{ m}$$
$$\dot{\boldsymbol{\rho}}_0(0) = [-0.3889, -0.4392, -0.8264]^T \text{ m/s} \tag{34}$$

$$\boldsymbol{\rho}_{10}(0) = [26.5, 26.5, 50]^T \text{ m}$$
$$\dot{\boldsymbol{\rho}}_{10}(0) = [-0.392, -0.4361, -0.8264]^T \text{ m/s} \tag{35}$$

and

$$\boldsymbol{\omega}(0) = [0.1n, 0.1n, 2n]^T \tag{36}$$

where $n = \sqrt{a_L^3/\mu} = 0.0596$ deg/s.

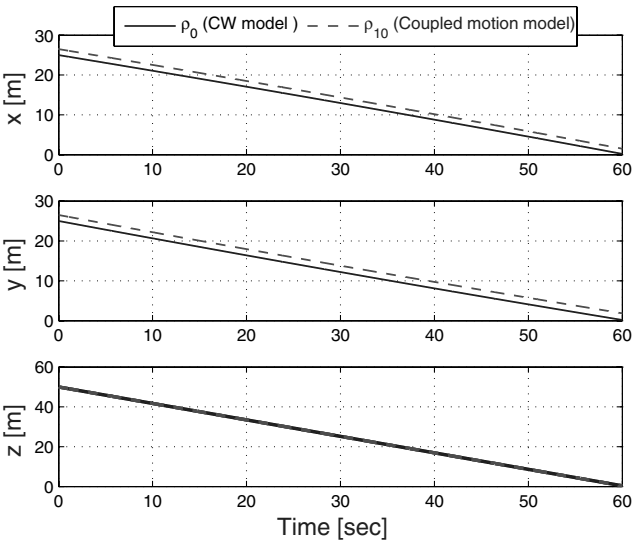

Fig. 4 Comparison between the relative position components as modeled by the Clohessy–Wiltshire and the approximate model (26) for a rendezvous mission.

The results of the rendezvous simulation are shown in Figs. 4 and 5. Figure 4 depicts the relative positions $\boldsymbol{\rho}_0$ and $\boldsymbol{\rho}_{10}$. Although the relative distance between the spacecrafts' centers of mass is decreasing to zero, the distance from the leader's c.m. to the point P_F^1 is not. Moreover, the normalized differences between model (26) and the CW model, defined as

$$\xi = \frac{x_{10} - x_0}{x_{10}}, \qquad \eta = \frac{y_{10} - y_0}{y_{10}}, \qquad \zeta = \frac{z_{10} - z_0}{z_{10}} \tag{37}$$

reaches 100% as $t \to t_f$, as can be seen in Fig. 5. Thus, this simulation clearly demonstrates that at the final approach phase of a rendezvous, the CW model will be invalid due to the kinematic coupling of rotation and translation.

V. Conclusions

In this paper, a kinematically coupled relative rotational and translational motion model, describing the 6 degrees-of-freedom relative dynamics between two rigid-body spacecraft was developed. The newly developed model generalizes the existing nonlinear relative-translation model to include trajectories of points that are not located on the spacecraft centers of mass. The relative motion of the non-c.m. points was illustrated by using two numerical simulations: a formation flying scenario and a rendezvous mission. The main observation is that neglecting the relative translation induced by the relative rotation can lead to considerable errors in distributed space systems flying in close proximity.

It was demonstrated that the points that are not located on the spacecraft c.m. are oscillating harmonically with respect to the leader spacecraft's c.m. This motion cannot be detected using traditional relative motion models. It was also shown that using the linear Clohessy–Wiltshire model can lead to considerable errors when applied to modeling of rendezvous and docking.

Orbital perturbations may induce differential dynamics that is more significant than the kinematic coupling effect. However, the latter effect is always present, even in short operation times (typical, for example, to orbital rendezvous), where orbital perturbations are less dominant. In fact, the kinematic coupling effect does not depend on environmental perturbations and is an inherent part of the nominal relative motion equations. As such, it should be taken into account in the linearized relative-translation equations.

References

[1] Kim, S., Crassidis, J. L., Cheng, Y., Fosbury, A. M., and Junkins, J. L., "Kalman Filtering for Relative Spacecraft Attitude and Position Estimation," *Journal of Guidance, Control, and Dynamics*, Vol. 30,

No. 1, Jan.–Feb. 2007, pp. 133–143.
doi:10.2514/1.22377

[2] Clohessy, W. H., and Wiltshire, R. S., "Terminal Guidance System for Satellite Rendezvous," *Journal of the Aerospace Sciences*, Vol. 27, No. 9, Sept. 1960, pp. 653–658.

[3] Lawden, D. F., *Optimal Trajectories for Space Navigation*, Butterworths, London, 1963, pp. 79–86.

[4] Carter, T., and Humi, M., "Fuel-Optimal Rendezvous Near a Point in General Keplerian Orbit," *Journal of Guidance, Control, and Dynamics*, Vol. 10, No. 6, Nov.–Dec. 1987, pp. 567–572.
doi:10.2514/3.20257

[5] Inalhan, G., Tillerson, M., and How, J. P., "Relative Dynamics and Control of Spacecraft Formations in Eccentric Orbits," *Journal of Guidance, Control, and Dynamics*, Vol. 25, No. 1, Jan.–Feb. 2002, pp. 48–60.
doi:10.2514/2.4874

[6] Alfriend, K. T., and Schaub, H. S., "Dynamics and Control of Spacecraft Formations: Challenges and Some Solutions," *Journal of the Astronautical Sciences*, Vol. 48, No. 2, April 2000, pp. 249–267.

[7] Kasdin, N. J., Gurfil, P., and Kolemen, E., "Canonical Modelling of Relative Spacecraft Motion via Epicyclic Orbital Elements," *Celestial Mechanics and Dynamical Astronomy*, Vol. 92, No. 4, 2005, pp. 337–370.
doi:10.1007/s10569-004-6441-7

[8] Gurfil, P., "Relative Motion Between Elliptic Orbits: Generalized Boundedness Conditions and Optimal Formationkeeping," *Journal of Guidance, Control, and Dynamics*, Vol. 28, No. 4, July–Aug. 2005, pp. 761–767.
doi:10.2514/1.9439

[9] Sabol, C., Burns, R., and McLaughlin, C. A., "Satellite Formation Flying Design and Evolution," *Journal of Spacecraft and Rockets*, Vol. 38, No. 2, March–April 2001, pp. 270–278.
doi:10.2514/2.3681

[10] Mishne, D., "Formation Control of Satellites Subject to Drag Variations and J_2 Perturbations," *Journal of Guidance, Control, and Dynamics*, Vol. 27, No. 4, July–Aug. 2004, pp. 685–692.
doi:10.2514/1.11156

[11] Pan, H., and Kapila, V., "Adaptive Nonlinear Control for Spacecraft Formation Flying with Coulped Translational and Attitude Dynamics," *Proceedings of the 40th IEEE Conference on Decision and Control*, Inst. of Electrical and Electronics Engineers, New York, Dec. 2001, pp. 2057–2062.

[12] Ploen, S. R., Hadaegh, F. Y., and Scharf, D. P., "Rigid Body Equations of Motion for Modeling and Control of Spacecraft Formations, Part 1: Absolute Equations of Motion," *Proceedings of the 2004 American Control Conference*, American Automatic Control Council, Evanston, IL, June 2004, pp. 3646–3653.

[13] Landau, L. D., and Lifshitz, E., *Mechanics*, Pergamon, Oxford, England, U.K., 1960, pp. 96–98.

[14] Gurfil, P., and Kholshevnikov, K. V., "Manifolds and Metrics in the Relative Spacecraft Motion Problem," *Journal of Guidance, Control, and Dynamics*, Vol. 29, No. 4, July–Aug. 2006, pp. 1004–1109.
doi:10.2514/1.15531